

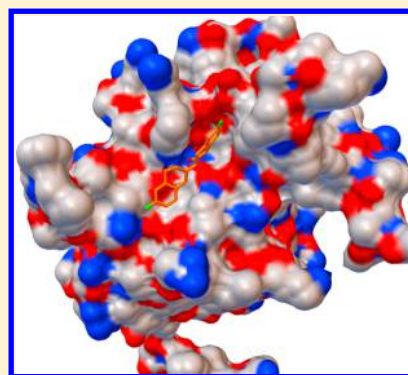
Identification of a Novel Inhibitor of Dengue Virus Protease through Use of a Virtual Screening Drug Discovery Web Portal

Usha Viswanathan,[†] Suzanne M. Tomlinson,[†] John M. Fonner,[‡] Stephen A. Mock,[‡] and Stanley J. Watowich^{*†}

[†]Department of Biochemistry and Molecular Biology, University of Texas Medical Branch, Galveston, Texas 77555, United States

[‡]Texas Advanced Computing Center, The University of Texas at Austin, Austin, Texas 78758, United States

ABSTRACT: We report the discovery of a novel small-molecule inhibitor of the dengue virus (DENV) protease (NS2B-NS3pro) using a newly constructed Web-based portal (DrugDiscovery@TACC) for structure-based virtual screening. Our drug discovery portal, an extension of virtual screening studies performed using IBM's World Community Grid, facilitated access to supercomputer resources managed by the Texas Advanced Computing Center (TACC) and enabled druglike commercially available small-molecule libraries to be rapidly screened against several high-resolution DENV NS2B-NS3pro crystallographic structures. Detailed analysis of virtual screening docking scores and hydrogen-bonding interactions between each docked ligand and the NS2B-NS3pro Ser135 side chain were used to select molecules for experimental validation. Compounds were ordered from established chemical companies, and compounds with established aqueous solubility were tested for their ability to inhibit DENV NS2B-NS3pro cleavage of a model substrate in kinetic studies. As a proof-of-concept, we validated a small-molecule dihydronaphthalenone hit as a single-digit-micromolar mixed noncompetitive inhibitor of the DENV protease. Since the dihydronaphthalenone was predicted to interact with NS2B-NS3pro residues that are largely conserved between DENV and the related West Nile virus (WNV), we tested this inhibitor against WNV NS2B-NS3pro and observed a similar mixed noncompetitive inhibition mechanism. However, the inhibition constants were ~10-fold larger against the WNV protease relative to the DENV protease. This novel validated lead had no chemical features or pharmacophores associated with adverse toxicity, carcinogenicity, or mutagenicity risks and thus is attractive for additional characterization and optimization.



I. INTRODUCTION

Virtual screening of small-molecule libraries has been a rewarding computational approach that leverages protein structural information and molecular docking algorithms to facilitate drug discovery.^{1–4} Although molecular docking algorithms use highly simplified empirical, force-field, or knowledge-based calculations^{5,6} to represent intermolecular interactions, these algorithms can often predict the conformation of a ligand bound to a protein's active site with high accuracy [e.g., root-mean-square deviation (rmsd) < 2 Å]. Moreover, for each bound conformation, the docking algorithms generate a "score" in an attempt to approximate the standard chemical potential of a ligand–protein interaction.

Virtual screening programs systematically perform docking calculations on a data set (or library) of small molecules to determine the conformation and molecular orientation that yields the most favorable score between each small molecule and a protein target. The scores are then sorted to produce a list of compounds predicted to bind with decreasing strength to a protein target. These predictions can be experimentally tested to identify and validate potential drug leads.⁷

To facilitate the discovery of novel drug leads and molecular probes, we developed a no-cost, globally accessible Web portal that can rapidly screen druglike commercially available small-molecule libraries and identify potentially tight-binding

protein–ligand complexes. The portal's interface was designed to allow intuitive and seamless access to current docking software, large virtual libraries, and powerful computational resources. Docking calculations were performed within AutoDock Vina,⁸ a program that had produced significant library enrichments against a number of protein targets. Its robustness was due in large part to a scoring function that combined empirical and knowledge-based scoring functions with empirical parameters derived from protein–ligand experimental binding affinities, interactions, and molecular conformations tabulated in the PDBbind data set.^{9,10} Virtual screening calculations were executed on supercomputers designed and maintained by the Texas Advanced Computing Center (TACC) at the University of Texas at Austin.

The World Health Organization has estimated that each year ~50–100 million people are infected with dengue virus (DENV), with ~2 million individuals developing clinical symptoms associated with dengue fever and dengue hemorrhagic fever.^{11,12} More recently, it was estimated that there were ~390 million DENV infections in 2010, of which ~96 million cases presented with clinical or subclinical symptoms.¹³ Although clinical trials are in progress, there are no approved

Received: September 2, 2014

Published: September 29, 2014



vaccines or therapies to treat or prevent DENV infections. An attractive target for selective antiviral therapeutics is the DENV serine protease (NS2B-NS3pro),¹⁴ since the U.S. Food and Drug Administration has approved several small-molecule protease inhibitors as antivirals for hepatitis C virus (HCV) and human immunodeficiency virus (HIV).^{15–17} Moreover, the DENV protease is essential for virus replication¹⁸ and highly conserved among all dengue strains and serotypes.¹⁹ Although substrate-based peptidic and small-molecule DENV protease inhibitors have been reported in the literature,^{20–26} to the best of our knowledge no DENV protease inhibitor has demonstrated antiviral efficacy in clinical trials.

Herein we describe the development of a Web portal for virtual drug discovery, its uniqueness, and its effectiveness in facilitating virtual docking studies. We leveraged this portal to rapidly identify potential inhibitors of DENV NS2B-NS3pro, using as targets several DENV protease crystallographic structures. Top-scoring hits from these virtual screening experiments were purchased from commercial vendors and validated in biochemical assays as inhibitors of recombinant DENV NS2B-NS3pro. As a proof-of-concept, we report on the validation of a dihydronaphthalenone lead as a low-micromolar noncompetitive inhibitor of DENV NS2B-NS3pro. Moreover, this small molecule also inhibited NS2B-NS3pro from the related West Nile flavivirus (WNV). This broad-spectrum lead had no pharmacophores associated with adverse toxicity, carcinogenicity, or mutagenicity risks and thus is attractive for additional development and optimization.

II. METHODS

Drug Discovery Portal. The Web-based drug discovery portal (Figure 1) was developed to provide a robust and intuitive interface to execute the Autodock Vina program on the “Lonestar” supercomputer, one of the high-performance computing resources designed, managed, and maintained by TACC (accessible through <https://portal.tacc.utexas.edu>). Lonestar is a high-performance computing cluster consisting of 23 844 processors and a peak processing speed of ~300 trillion floating point operations per second (TFlops). The portal, termed DrugDiscovery@TACC, was coded to enable users to upload a target structure against which docking calculations can be performed. The target structure file can be provided in either Protein Data Bank (PDB) format^{27–29} or PDBQT format (a modified PDB file that includes the partial charge and AutoDock atom type for each listed atom). Uploaded PDB-formatted files are automatically converted to the PDBQT format required by the Autodock Vina program. In addition to the target structure, only a small number of user-supplied inputs are required to initiate a virtual screening experiment. These inputs include the center of the search space used for docking calculations, the size of the search space examined during the docking calculations, and specification of the virtual library chosen for screening from among the set of supplied libraries (discussed below).

Upon successful entry of all required input parameters, the portal creates a configuration file for the Autodock Vina application as well as a bundle of scripts needed for the docking phase and the postprocessing phase of job execution. This application bundle is copied from the portal host to Lonestar and unpackaged, and the two jobs are submitted to the Sun Grid Engine queuing system responsible for scheduling jobs on Lonestar. The jobs transmit state notifications back to the portal, enabling the portal to communicate job status to the

user and allow the user to abort the job if necessary. When the portal receives notification that a run is completed, it unstages the result files back to the portal's disk storage area and provides a link that enables the results to be downloaded to local computers in a compressed (zip) format. The downloaded results include a Vina configuration file, a protein target file in PDBQT format, a listing of the 1000 best-scoring (i.e., lowest docking score) ligands with their corresponding scores, and 1000 individual PDB-formatted files containing the most favorable conformation and orientation of the best-scoring ligands.

Protease Sequence Alignment. Protein sequences for the NS3 protein from DENV and WNV strains were obtained from the NIH Virus Variation site (www.ncbi.nlm.nih.gov/genomes/VirusVariation). For DENV serotypes 1–4, totals of 829, 796, 513, and 73 sequences, respectively, were selected and compared. Additionally, 55 WNV sequences isolated from human samples collected in North America were aligned and compared. Separate consensus sequences were produced for each DENV serotype and WNV using the program CLC Sequence Viewer (version 6.1; CLCbio, Cambridge, MA). The alignments were saved as FASTA-formatted files and manually edited to include only the protease regions (residues 1–185) of the NS3 protein. The Geneious program (Geneious Basic 5.0.3; Biomatters Ltd., Auckland, New Zealand) was used to interpret sequence variation and produce alignment figures. Sequence conservation was computed by visual inspection of the NS3 protease domain (residues 1–182) and the protease active site (defined as residues within 8 Å of C β atoms of the His51, Asp75, Ser135 catalytic triad in the 3U1J PDB structure).

Target Preparation. Three different crystallographic DENV protease structures, corresponding to inhibitor-free and inhibitor-bound NS2B-NS3pro enzymes, were used as targets for virtual screening. The ligand-free protease structure (PDB identifier 2FOM³⁰) consisted of a hydrophilic region of NS2B (residues 43–96) linked to the NS3 protease domain (residues 1–185); the amino sequence corresponded to DENV serotype 2 (DEN2V). The inhibitor-bound protease structures (PDB identifiers 3U1I and 3U1J³¹) consisted of NS2B residues 45–95 linked to residues 1–182 of the NS3 protease domain. The amino acid sequences of 3U1I and 3U1J were identical and corresponded to DENV serotype 3 (DEN3V). Cocrystallized with the DENV protease were either a small tetrapeptide inhibitor (3U1I structure) or aprotinin (a polypeptide also known as bovine pancreatic trypsin inhibitor; 3U1J structure). No bound water molecules were observed to mediate interactions between aprotinin and the DENV protease (3U1J structure). Only a single water molecule was observed to potentially mediate interactions between the tetrapeptide inhibitor and the DENV protease in the 3U1I structure. However, the angle between the carbonyl oxygen of the OAR5 group of the tetrapeptide inhibitor and the water molecule (HOH 206) was ~101°, which suggested that this interaction was very weak or not significant. Thus, all of the crystallographic waters and inhibitors were manually removed from the PDB files prior to the screening experiments. AutoDockTools³² software (<http://mgltools.scripps.edu>) was used to add polar hydrogens, protonate the N δ atom of His51, specify AutoDock4 atom types, and convert PDB files to PDBQT file formats; comparable results were obtained when target protein structures were prepared automatically using portal software (data not shown).

Virtual screenings against the inhibitor-bound protease structures (PDB 3U1I and 3U1J) were performed using a search box with dimensions of $28 \text{ \AA} \times 28 \text{ \AA} \times 28 \text{ \AA}$. However, using this search grid size with the inhibitor-free protease structure (PDB 2FOM) resulted in a significant number of high-scoring ligands being placed in a channel $\sim 11 \text{ \AA}$ distant from the catalytic triad. Thus, a $22 \text{ \AA} \times 22 \text{ \AA} \times 22 \text{ \AA}$ box was used when performing virtual screens against the 2FOM target protein; in these calculations, all of the examined high-scoring ligands were positioned in the protease active site. These search boxes, centered on either Ser135 or His51, were of sufficient size to cover much of the binding site that is unique to DENV proteases and that is involved in binding of a tetrapeptide inhibitor (as defined by the cocrystal structure of PDB 3U1I).

Residues His51, Asp75, and Ser135 of the NS3 structure form the prototypical catalytic triad observed in serine proteases. To examine the influence of the coordinate chosen for the search box center, separate screening experiments were performed using either the N δ atom of His51 or the O γ atom of Ser135 as the center of the docking search space. These coordinates differed by $\sim 5 \text{ \AA}$.

Library Preparation. Two virtual libraries containing commercially available small molecules were compiled for use with the Web-based drug discovery portal. The larger data set of compounds, termed the “collective” library, was a subset of the ZINC database³³ with “clean, druglike” constraints that required molecules to have the following properties: molecular weight between 150 and 500 Da, $\text{clogP} \leq 5$, five or fewer hydrogen-bond donors, and 10 or fewer hydrogen-bond acceptors. This data set was additionally filtered to include only compounds that were available for purchase from either ChemBridge Corporation (San Diego, CA), ChemDiv Inc. (San Diego, CA), Ryan Scientific Inc. (Mount Pleasant, SC), Maybridge Chemical Company (Cambridge, U.K.), or Sigma-Aldrich (St. Louis, MO), since these vendors have supplied milligram quantities of chemicals for biochemical assays reliably, rapidly, and at low cost. A total of 642 769 druglike commercially available small molecules were included in the collective library.

A second “focused” library was constructed by applying clogP filters to druglike compounds available from ChemBridge and Maybridge Chemical. This filter was designed to improve the likelihood that available compounds would be soluble in aqueous solutions and suitable for biochemical assays. Chemicals available from ChemBridge were filtered to retain only “druglike” compounds with the following properties: $\text{clogP} < 1.0$, zero net charge, fewer than nine rotatable bonds, fewer than 11 H-bond acceptors, and molecular weights between 250 and 600 Da. Compounds from Maybridge Chemical were similarly filtered, although compounds with $\text{clogP} < 1.8$ were retained. Additionally, the focused library included 14 400 unique small molecules from the Maybridge HitFinder V10 data set that is widely used for experimental high-throughput screening studies. Property filters were not applied to the HitFinder library, to mimic the commercially available library commonly used for small-scale high-throughput screening. In total, the focused library contained 45 458 small-molecule structures (after elimination of 1493 duplicate ligands). MOL2 files for these compounds were obtained from the ZINC database and converted to PDBQT format using the “prepare ligand” module available in the AutoDockTools package (<http://mgltools.scripps.edu>).

Drug discovery jobs that specified the collective or focused library for virtual screening were allocated 1920 and 480 processors, respectively, on the Lonestar cluster for job execution.

Expression and Purification of DENV Protease. The DEN2V protease (plasmid construct *CF40-Gly-NS3pro185*) was expressed in *Escherichia coli* largely following the previously described protocol,¹⁹ although cell growth was continued for 8 h at 25°C following the addition of 0.4 mM isopropyl D-thiogalactopyranoside (IPTG). Purification was performed as described previously^{3,25,34} using metal affinity chromatography. Purified, concentrated NS2B-NS3pro was stored at -80°C in cleavage buffer (200 mM Tris, pH 9.5, 20% glycerol). The activity of the dengue protease was not impacted by a freeze/thaw cycle (data not shown).

Expression and Purification of WNV Protease. Recombinant WNV protease was expressed in *E. coli* and purified to homogeneity following the previously described protocol.³⁵

Protease Inhibition Assays. Small molecules identified by virtual screening as potential DEN2V protease inhibitors were tested for inhibition activity using NS2B-NS3 protease steady-state kinetic assays as described previously.^{3,25,34,35} Briefly, compounds identified in virtual screening experiments were received from established chemical vendors and tested for solubility at 10 mM in dimethyl sulfoxide (DMSO) and upon 100-fold dilution from DMSO into cleavage buffer (final DMSO concentration of 1%); solubility tests included centrifugation, comparison of absorption curves pre- and postfiltration through $0.22 \mu\text{m}$ filters, and establishment of linear absorption calibration curves. Sequential 10-fold serial dilutions and calibration curves were used to determine the limits of solubility in cleavage buffer as necessary.

Preliminary single-point inhibition assays^{3,25,34} were used to check the activities of compounds using 100 nM NS2B-NS3 and 100 μM substrate in cleavage buffer for 30 min at 25°C . DENV and WNV protease assays were performed with Boc-GRR-AMC and Boc-GKR-AMC fluorogenic substrates (Bachem America Inc., Torrance, CA), respectively. Fluorescence measurements were performed in duplicate on a Fluorolog FL3-22 spectrofluorometer (Horiba Jobin Yvon) and corrected for compound absorption and emission. Compounds that demonstrated protease inhibition (defined as a 25% reduction in protease activity relative to the control) in preliminary studies were tested in detailed kinetic assays using a range of substrate concentrations (1200, 600, 300, 150, 75, and 37.5 μM) and 100 nM NS2B-NS3 in cleavage buffer at 25°C . All of the experiments were performed using two different inhibitor concentrations and a “no inhibitor” control. Fluorescence measurements were recorded at 5 min intervals from 0 to 30 min. Fluorescence intensities were converted to AMC product concentrations using calibration curves established in the presence of the inhibitor. The initial velocity at each substrate concentration was calculated using linear curve fits of AMC production per unit time using replicate measurements and the program GraphPad Prism 4 (Graphpad, San Diego, CA). The program Dynafit (Biokin, Watertown, MA)^{36–38} was used to compare Michaelis–Menten inhibition models and calculate catalytic parameters that produced the best fits to the measured velocity versus substrate kinetic data collected with no inhibitor present. To determine inhibition parameters and mechanism of action, the kinetic parameters were held constant and the inhibition parameters were adjusted to provide an optimal

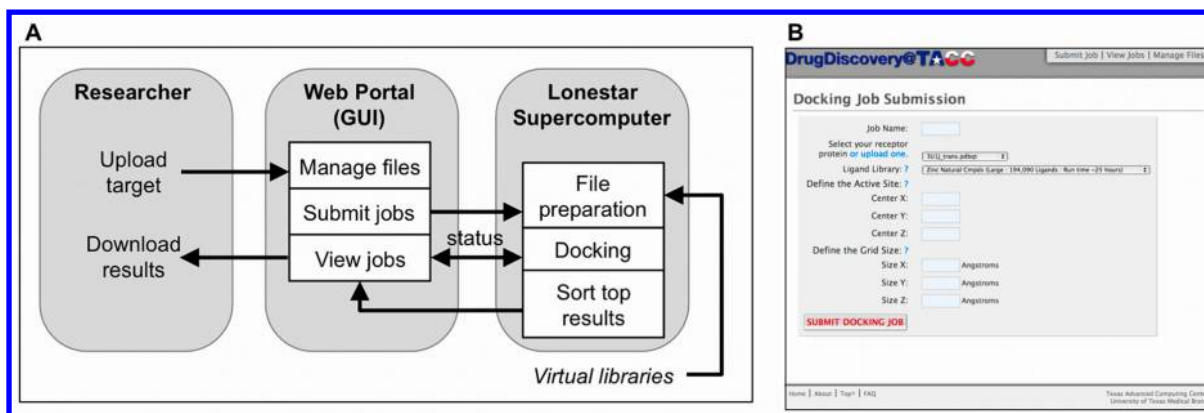


Figure 1. (A) Schematic diagram of the underlying workflow structure of the TACC drug discovery portal and (B) a screenshot of the intuitive graphical user interface used to input all of the parameters necessary to initiate a virtual drug discovery experiment.

global fit to velocity versus substrate data sets collected at three inhibitor concentrations (including no inhibitor). Comparable experimental and data analysis approaches have been described in great detail in previous publications.^{25,35}

III. RESULTS AND DISCUSSION

Portal Implementation. The DrugDiscovery@TACC portal (Figure 1) was established to provide a robust, easy-to-use resource for structure-based virtual screening of large libraries of druglike commercially available small molecules. This portal, backed by massive computational resources, greatly extends the capabilities of existing Web portals that either perform molecular docking between a user-supplied protein target and ligand [e.g., Patchdock (<http://bioinfo3d.cs.tau.ac.il/PatchDock>), ParDOCK (<http://www.scfbio-iitd.res.in/dock/pardock.jsp>), and SwissDock (<http://swissdock.vital-it.ch/docking>)], screen a portal-supplied small library (e.g., iScreen³⁹), or screen a small user-supplied ligand library (e.g., DOCK Blaster⁴⁰). In addition, this portal was designed to be freely available to both academic and nonacademic researchers and thus provides resource-limited researchers with an alternative to fee-based virtual screening services.

The DrugDiscovery@TACC portal (accessible at <https://drugdiscovery.tacc.utexas.edu>) was implemented by a team of computer specialists at TACC. Access to portal resources and user files is controlled by username and password authentication, which are obtained in a two-step procedure. First, an account must be requested directly from TACC (<https://portal.tacc.utexas.edu/account-request>) to comply with their security practices and monitor usage of government-funded computational resources. Users can be affiliated with educational or commercial organizations located in the United States or other countries. Account requests are typically approved, unless the request is prohibited by United States export control regulations or involves a "Country of Concern" listed on United States or international sanctions and embargo list. Once a TACC user account is established, each user is provided with private file storage for uploaded target proteins and screening calculation results. However, a portal-wide CPU allocation is debited during execution of drug discovery calculations. This hierarchy provides users with seamless access to TACC resources and shields them from project administrative tasks. Once logged into the portal, users interact with a simple graphical user interface (GUI) to submit new jobs, view job status, and manage files (Figure 1B). To submit a new drug

discovery project, the following information is entered through the GUI: a unique job name, a file containing the target protein coordinates (in either PDB or PDBQT format), the library for screening (selected from portal options through a pull-down menu), the coordinates of the search box center (typically within the protein's active site), and the search box dimensions. Portal-supplied libraries include the collective library [referenced as "Zinc(Large 642,759 Ligands)"] and the focused library [referenced as "Zinc(Small 46,702 Ligands)"], as described in Methods. The "Manage Files" tab enables protein coordinate files to be uploaded to TACC disk servers, completed jobs to be downloaded to local storage, and files stored on TACC disk servers to be deleted.

A single docking calculation between a protein target and a single small, flexible ligand requires 1–3 min of processing time on a single CPU core of the Lonestar supercomputer hosting the DrugDiscovery@TACC portal; computer times are dependent on the ligand size, the number of ligand rotatable bonds, and the size of the search grid volume. Search "exhaustiveness" (a Vina parameter) was set at a value of 10, which produced reproducible poses from multiple simulations. Higher values of the exhaustiveness level increased the processing time without changing the resulting docked conformation, orientation, and docking score.

Drug discovery projects screening the collective library are assigned 1920 processors, enabling most projects to be completed within 8–12 h. For comparison, screening a similar-sized library on a current-generation personal computer would require over a year of dedicated computer time. Drug discovery projects screening the focused library are assigned 480 processors, enabling most projects to be completed within 2 h. The slightly longer average execution time per processor per ligand observed for the collective library relative to the focused library reflects the nonlinear increase in data management time required for the large collective library. Multiple drug discovery projects can be performed concurrently. Heavy system loads increase the time a job remains in the Lonestar queue before beginning execution, which could increase the time needed to complete a job by several hours. At the time of writing, the DrugDiscovery@TACC portal had completed over 2.5 million CPU hours of docking calculations for ~80 different researchers internationally.

Virtual Screening against Dengue Virus Protease Structures. Four major DENV serotypes and thousands of different DENV strains exist. Comparison of NS3 protease sequences from 2211 different DENV strains from serotypes

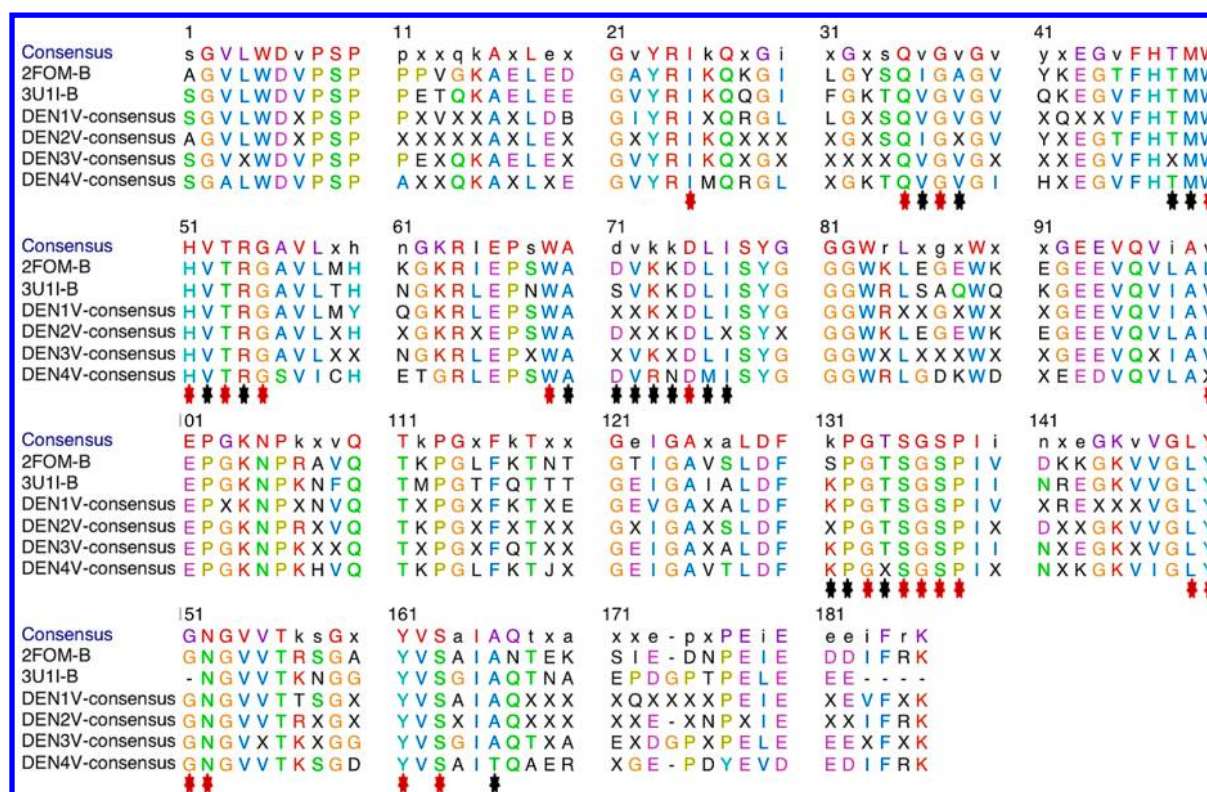


Figure 2. Sequence alignment between NS3pro structures (chain B) used for crystal studies (PDB structures 2FOM and 3U1I/3U1J) and consensus sequences produced from analysis of 829, 796, 513, and 73 sequences from DENV serotypes 1–4, respectively. The same protein sequence generated PDB structures 3U1I and 3U1J. For the consensus sequences, serotype sequences were obtained from the NIH Virus Variation site (www.ncbi.nlm.nih.gov/genomes/VirusVariation) and aligned using the program CLC Sequence Viewer (version 6.1; CLCbio, Cambridge, MA). Each “X” denotes a sequence location that was not conserved within a serotype. The consensus sequence and final figure were produced using the Geneious program (Geneious Basic 5.0.3; Biomatters Ltd., Auckland, New Zealand). Stars highlight residues within 8 Å of the protease catalytic triad (termed active-site residues); red-colored stars identify active-site residues that are conserved among all of the examined DENV and WNV sequences.

1–4 showed that ~40% of the residues were invariant (Figure 2). However, the NS3 protease active site was more conserved relative to the entire NS3 protease domain, with ~66% sequence identity for active-site residues from 2211 DENV NS3 protease sequences (Figure 2). In addition, several structures of the DENV protease have been determined under different crystallographic conditions. Since rapid docking algorithms, including AutoDock Vina, treat protein targets as rigid entities, small changes in target conformation and/or sequence can dramatically modify virtual screening results. To improve the likelihood of identifying promising protease inhibitors, independent virtual screening experiments were performed against NS2B-NS3 protease structures from DENV serotypes 2 (PDB reference identifier 2FOM) and 3 (PDB reference identifiers 3U1I and 3U1J) to sample varied conformational and sequence space. The 2FOM and 3U1J (or 3U1I) NS3 protease sequences were ~70% identical, and their active-site residues had ~90% sequence identity (Figure 2). The target NS2B-NS3pro structures had significantly different protein backbone conformations (Figure 3A–C), side-chain positions, and active-site surfaces (Figure 3D–F). In particular, the NS2B polypeptide adopted different conformations in response to being crystallized as an unbounded enzyme (2FOM structure) or with a tetrapeptide (3U1I structure) or small protein (3U1J structure) inhibitor. The NS2B did not adopt a consistently unique conformation (e.g., a “closed” conformation⁴¹) when bound to an inhibitor, since the two

protease–inhibitor cocrystal structures had significantly different NS2B conformations³¹ (Figure 3A).

Vina was tested against a number of serine protease cocrystal structures that enabled us to validate its ability to reproduce crystallographic structures [e.g., the lowest-energy pose for Vina docking of 1-(4-aminophenyl)-3-(4-chlorophenyl)urea to trypsin reproduced the cocrystal structure 1BJU with an rmsd of 0.55 Å; see also Trott and Olson⁸]. When applied to the DENV protease structures, Vina virtual screening produced a list of hits that were then sorted by docking score; a more negative score was assumed to correspond to more favorable energetic interactions between a ligand and the target protein. Hits were classified as “high-scoring” if they had a docking score below an arbitrary cutoff value chosen to select a manageable number of ligands (e.g., 20–60) from each virtual screen for subsequent analysis and validation experiments. High-scoring hits were parsed through the ZINC database to remove identical compounds with different ZINC identifiers. Screens initiated with different search box centers did not produce identical sets of high-scoring hits; instead, screens with different search volume centers were observed to have only 40–80% of their ligands in common (Figure 4). Since the reproducibility of docking scores was approximately ± 0.1 units, some hits that were unique to one search box center screen appeared in other hit lists just below the defined cutoff value. However, many ligands had docking scores that differed substantially among virtual screens performed with different search box centers. Thus, screening around several search volume centers had a

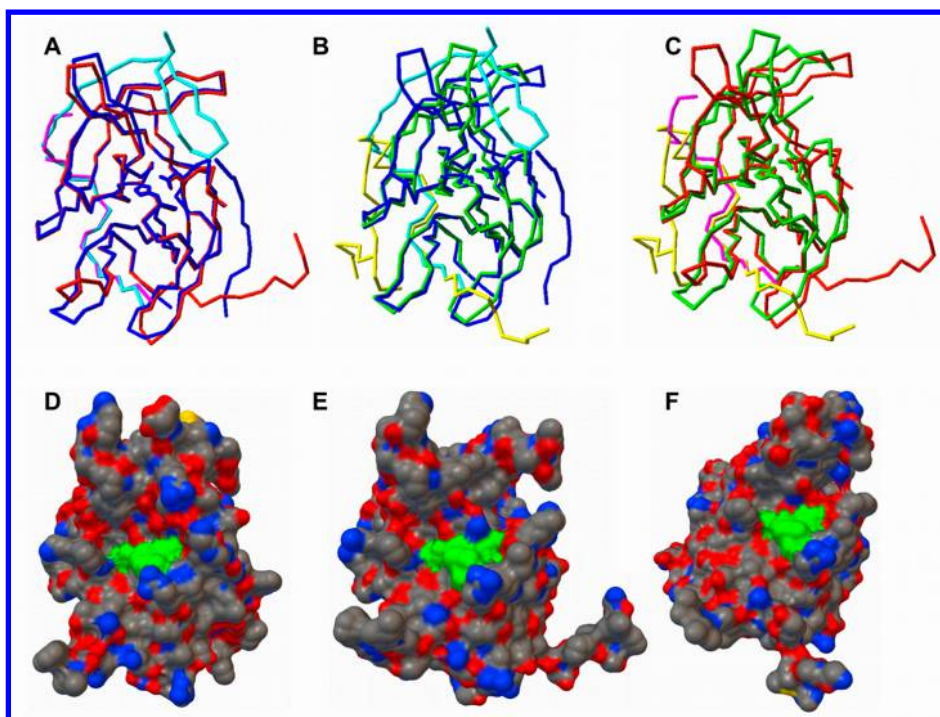


Figure 3. (A–C) Comparisons of the DENV NS2B-NS3pro structures used as targets for virtual screening: (A) overlaid $C\alpha$ traces of PDB structures 3U1I and 3U1J; (B) overlaid $C\alpha$ traces of PDB structures 3U1I and 2FOM; (C) overlaid $C\alpha$ traces of PDB structures 3U1J and 2FOM. In 3U1I, the NS2B and NS3pro chains are colored cyan and blue, respectively. In 3U1J, the NS2B and NS3pro chains are colored magenta and red, respectively. In 2FOM, the NS2B and NS3pro chains are colored yellow and green, respectively. (D–F) Surface representations of PDB structures (D) 3U1I, (E) 3U1J, and (F) 2FOM. The surfaces are colored gray, red, and blue to indicate surface areas formed by carbon, oxygen, and nitrogen atoms, respectively. The green-colored areas indicate the location of catalytic residue His51. Images were prepared with the molecular graphics programs Swiss-PDBViewer⁴⁸ and PyMOL.⁴⁹

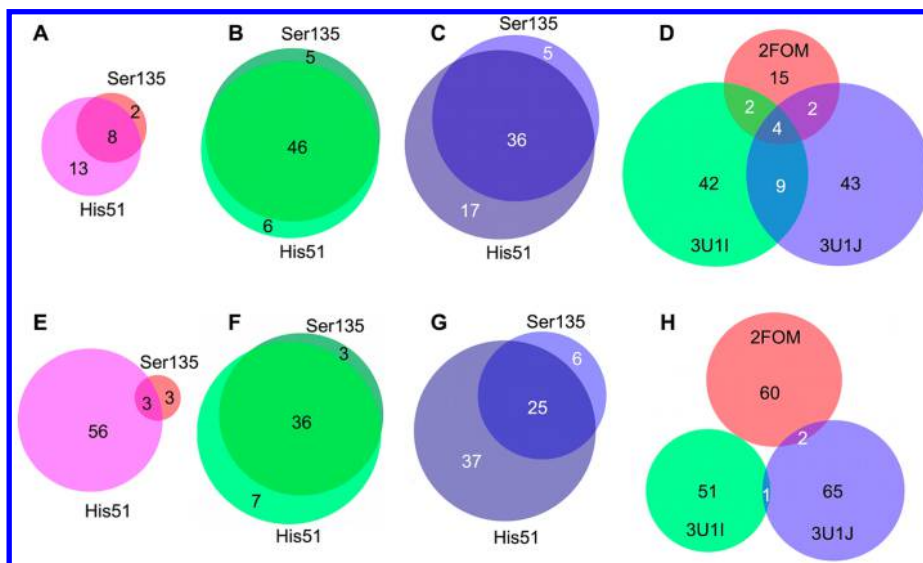


Figure 4. Venn diagrams representing the overlap between high-scoring hits identified in independent virtual screens. (A) Number of high-scoring hits (docking scores from -11.0 to -8.8) identified from screening of 2FOM against the focused library using search volumes centered on His51 and Ser135. (B) Number of high-scoring hits (docking scores from -10.0 to -9.0) identified from screening of 3U1I against the focused library using search volumes centered on His51 and Ser135. (C) Number of high-scoring hits (docking scores from -10.4 to -9.0) identified from screening of 3U1J against the focused library using search volumes centered on His51 and Ser135. (D) Number of high-scoring hits in common from virtual screens of 2FOM, 3U1I, and 3U1J against the focused library. (E) Number of high-scoring hits (docking scores from -10.4 to -9.6) identified from screening of 2FOM against the collective library using search volumes centered on His51 and Ser135. (F) Number of high-scoring hits (docking scores from -10.3 to -9.9) identified from screening of 3U1I against the collective library using search volumes centered on His51 and Ser135. (G) Number of high-scoring hits (docking scores from -10.7 to -9.9) identified from screening of 3U1J against the collective library using search volumes centered on His51 and Ser135. (H) Number of high-scoring hits in common from virtual screens of 2FOM, 3U1I, and 3U1J against the collective library. Area-proportional Venn diagrams were produced using the program BioVenn.⁵⁰

clear benefit in being able to identify a wide range of high-scoring hits.

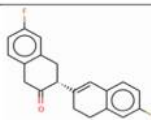
Unique high-scoring hits from virtual screens performed with Ser135 and His51 as search volume centers were merged into a single set of hits for each protein target and library combination. This produced six hit lists for further analysis. Most of the hits were unique to a specific combination of protein target and library (Figure 4D,H). A total of 117 high-scoring hits were identified from virtual screening experiments with the smaller focused library; 100 of these hits (85%) were unique to a single protein target (15 hits unique to 2FOM, 42 hits unique to 3U1I, and 43 hits unique to 3U1J). Only four hits were common to all of the proteins that were screened against the focused library (Figure 4D). A total of 179 high-scoring hits were identified from virtual screening experiments with the collective library; all but three hits were unique to a single protein target (60 hits unique to 2FOM, 51 hits unique to 3U1I, and 65 hits unique to 3U1J) (Figure 4H). No hits were common to all of the proteins that were screened against the collective library (Figure 4H). It is clear that independent targets produce distinct hit lists, and a priori it is difficult to select a “best” target from all of the available structures for virtual screening experiments. Thus, the DrugDiscovery@TACC portal provides the computational resources to rapidly screen a large number of equally valid targets.

High-scoring hits were searched against the ZINC database to validate that library compounds were still listed in the continually updated ZINC database; this step removed ~8% of the hits from the collective library (leaving 164 high-scoring hits). The number of high-scoring hits contributed by the focused library remained unchanged.

In view of the large number of high-scoring hits identified at this point, an analysis of predicted molecular interactions between the protease targets and docked ligands was completed to reduce the number of hits that would be purchased and validated in protease inhibition assays. High-scoring hits were removed from further consideration if they did not hydrogen-bond to at least one of the catalytic site residues. In addition, hits were discarded if they had poor predicted solubility (ZINC12367578, 1-[(9,10-dioxo-9,10-dihydroanthracen-1-yl)-thio]-9,10-dihydroanthracene-9,10-dione), contained few heteroatoms (e.g., ZINC 3126348, 2-[(1-cyano-3-phenanthryl)-methyl]phenanthrene-1-carbonitrile), were planar (e.g., ZINC59593469, 2-(7H-benzo[c]fluoren-7-ylidenemethyl)-fluoranthene), and/or contained a formal charge (e.g., ZINC5830003, 5-amino-5-deoxyglucopyranose bisulfite).

Preliminary Inhibition Screen and Kinetic Assay. Small molecules identified from the above virtual screenings and property-filtering steps were purchased from chemical vendors and tested in solubility, single-point protease inhibition, and protease kinetic assays. We report proof-of-concept results for the validated compound ZINC04321905 (Table 1); this compound was a member of the focused library and was identified as the 14th best-scoring hit (docking score = −9.1, relative to the lowest score of −10.0) when this library was screened with a 3U1J target centered on Ser135 and as the 20th best-scoring hit when screened with a 3U1J target centered on His51 (docking score = −9.2, relative to the top score of −10.4). In both screening experiments, This ligand was ranked as the ~200th hit when the focused library was screened with the 2FOM DENV protease structure (docking score = −8.0, relative to the top score of −11.0) and was not in the top 500 hits when the focused library was screened against the 3U1I

Table 1. Structure and Calculated Inhibition Constants for ZINC04321905 against DENV and WNV NS2B-NS3 Proteases

Structure	Inhibition constants (μM)	
	DENV	WNV
	$K_{i1} = 7 \pm 1^{a,b}$	$K_{i1} = 71 \pm 21^{a,b}$
	$K_{i2} = 15 \pm 3^a$	$K_{i2} = 3.9 \pm 0.2^a$
	$K_{is} = 1130 \pm 360^b$	$K_{is} = 44 \pm 14^b$

^aDerived from the mixed noncompetitive substrate inhibition model (Figure 5B). ^bDerived from the modified competitive substrate inhibition model (Figure 5C).

structure. A more detailed study of all the identified inhibitors is beyond the scope of this article and will be presented in the future.

Catalytic parameters and inhibition constants were calculated using simultaneous nonlinear regression fitting of a generalized Michaelis–Menten model to velocity versus substrate concentration data collected from DENV protease reactions. This curve-fitting approach for analyzing kinetic data has been shown to (1) generate more accurate catalytic and inhibition parameters compared with reciprocal plots of closed-form solutions (e.g., Lineweaver–Burk, Dixon plots) to simple reaction models, (2) enable novel reaction models to be systematically generated, and (3) provide a rigorous approach for comparing alternative reaction models.^{35,36,38,42,43} A best fit to the DENV protease data (Figure 5A) was achieved using either a mixed noncompetitive substrate inhibition model (Figure 5B) with catalytic parameters $k_{cat} = 0.0065 \text{ s}^{-1}$, $K_d = 540 \text{ μM}$, and $K_{d2} = 4740 \text{ μM}$ and inhibition constants $K_{i1} = 7 \text{ μM}$ and $K_{i2} = 15 \text{ μM}$ (Table 1) or a modified competitive substrate inhibition model (Figure 5C) with the same catalytic parameters as noted above and inhibition constants $K_{i1} = 7.3 \text{ μM}$ and $K_{is} = 1130 \text{ μM}$ (Table 1). These reaction models and associated catalytic parameters were similar to those in previous DENV NS2B-NS3pro kinetic studies.^{25,35} Reaction curves generated with these parameters and either inhibition model produced excellent global fits to the experimental kinetic data (Figure 5A), indicating that these models were consistent with the experimental data. Simple competitive and uncompetitive inhibition models were not consistent with the data (data not shown). This approach to kinetic analysis has been the foundation of kinetic studies from the earliest days.^{44–47} The mixed noncompetitive substrate inhibition model and the modified competitive substrate inhibition model are thermodynamically equivalent and form a closed thermodynamic cycle if the states ESI and EIS* freely interconvert. The modified competitive substrate inhibition model provides an easily understood structural interpretation of the inhibition mechanism, suggesting that the AMC-linked tripeptide substrate can bind at two interacting sites on the protease (termed S and S* in Figure 5C) with the ZINC04321905 inhibitor competing for binding at the S site. Binding of an inhibitor or substrate to the S site facilitates binding of a substrate molecule to the S* site. Structural studies will be required to fully probe this interpretation.

Potential druglike properties of ZINC04321905 were calculated using the OSIRIS property calculator (<http://www.organic-chemistry.org/prog/peo>), which suggested that this small molecule does not contain pharmacophores associated

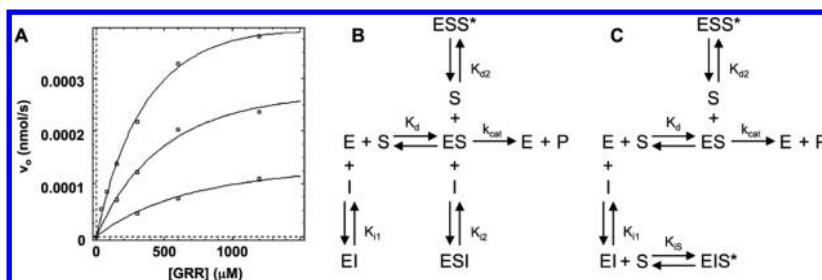


Figure 5. Global curve fitting of Michaelis–Menten reaction models to kinetic inhibition data for DENV protease cleavage of the Boc-GRR-AMC substrate. (A) Data points were collected for protease reactions performed with ZINC04321905 at concentrations of 0 (top curve), 7.5 (middle curve), and 35 μM (bottom curve). Data were analyzed with the program Dynafit according to a Michaelis–Menten reaction mechanism with substrate inhibition and either (B) mixed noncompetitive ligand inhibition or (C) modified competitive ligand inhibition. As discussed in the text, reaction models B and C both generate the curves shown in panel A. Initial velocity data points showed <2% error.

with increased risk of adverse mutagenic, tumorigenic, or irritant effects. However, the double bond in the cyclohexane ring has been associated with increased risk of adverse reproductive effects. This information can guide analogue design directed toward replacing nondruglike molecular fragments of ZINC04321905 with druglike molecular groups.

Vina docking calculations predicted ZINC04321905 to interact with the DENV protease in a manner similar to the binding conformation of the terminal arginine moiety identified from cocrystal studies of DEN3V NS2B-NS3pro and a tetrapeptide inhibitor (Figure 6). This predicted interaction is

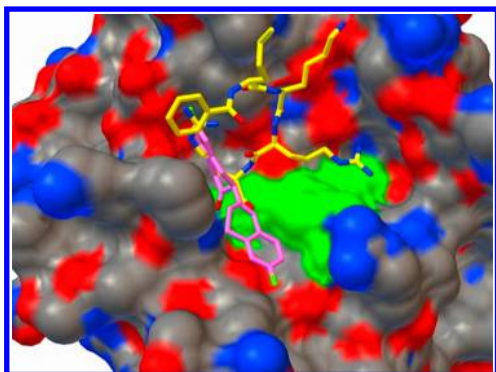


Figure 6. Inhibitor binding to DEN3V NS2B-NS3pro. The orientation of the ligand ZINC04321905 (magenta-colored bonds) bound to DEN3V protease (PDB structure 3U1J) was calculated by the Vina docking program; similar ligand orientations and conformations were calculated with protein targets 3U1I and 2FOM. The costructure of a tetrapeptide inhibitor (yellow carbon bonds) bound to the DEN3V protease (based on PDB structure 3U1I) is shown for comparison. The molecular surface formed by DEN3V protease is colored gray, blue, and red to reflect the underlying carbon, nitrogen, and oxygen atoms, respectively. The molecular surface of the catalytic triad (His51, Asp75, Ser135) is colored green. The image was prepared with PyMOL.⁴⁹

consistent with the inhibitor-binding mode (i.e., the S site) suggested in the above discussion of the modified competitive substrate inhibition model. The predicted binding orientation enables ZINC04321905 to form several hydrogen bonds to backbone amides of Gly133, Thr134, and Ser135 (Figure 7A) and interact with a large apolar pocket adjacent to Ser135 (Figures 6 and 7A). The residues forming the ZINC04321905 binding surface are highly conserved in DENV serotypes. Vina docking calculations predict ZINC04321905 to bind in similar orientations and conformations to different DENV serotype

proteases (PDB structures 3U1J and 2FOM) (Figure 6; data not shown). Ten of the 11 DENV protease residues predicted to interact with ZINC04321905 are conserved in the 2211 DENV strains examined (Figure 2), suggesting that this small molecule could be a pan-dengue protease inhibitor; future studies with DENV serotypes 1, 3, and 4 will address this hypothesis.

Residues that form the ZINC04321905 binding surface and the protease active site (i.e., residues within 8 Å of the catalytic triad) are largely conserved (>55% sequence identity) between DENV and WNV proteases, suggesting that ZINC04321905 could bind to the WNV protease. Vina docking calculations supported this suggestion and predicted ZINC04321905 to bind similarly to WNV NS2B-NS3pro (PDB structure 2FP7³⁰) and DEN3V NS2B-NS3pro (PDB structure 3U1J) and make a number of similar intermolecular contacts (Figure 7). Thus, inhibition studies of WNV protease were performed to determine whether ZINC04321905 could inhibit proteases from closely related flaviviruses. With recombinant WNV NS2B-NS3pro and Boc-GKR-AMC fluorogenic peptide substrate, kinetic data were collected at multiple substrate and ZINC04321905 concentrations as described previously.³⁵ Catalytic parameters and inhibition constants were calculated from global fitting of a generalized Michaelis–Menten model to the WNV kinetic data, and the best fit (data not shown) was achieved using a mixed noncompetitive substrate inhibition model with catalytic parameters $k_{\text{cat}} = 0.073 \text{ s}^{-1}$, $K_{\text{d}} = 800 \mu\text{M}$, and $K_{\text{d2}} = 592 \mu\text{M}$ and inhibition constants $K_{\text{i1}} = 71 \mu\text{M}$ and $K_{\text{i2}} = 3.9 \mu\text{M}$ (Table 1). Thus, ZINC04321905 functions as a WNV protease inhibitor, although it exhibits ~10-fold weaker binding to the WNV protease relative to the DEN2V protease. This decreased binding affinity may result from the smaller number of intermolecular interactions and hydrogen bonds predicted to form between ZINC04321905 and the WNV protease relative to the interactions predicted to form between ZINC04321905 and the DEN2V protease.

IV. CONCLUDING REMARKS

This project demonstrated the successful application of a powerful drug discovery portal to identify leads for further development. The portal provides access to the supercomputer resources of the Texas Advanced Computing Center to rapidly screen several integrated libraries containing almost a million druglike ligands. Ease of access and rapid turnaround times enable researchers with a wide range of computational expertise to perform numerous virtual screening experiments against macromolecular targets. Compounds contained within these

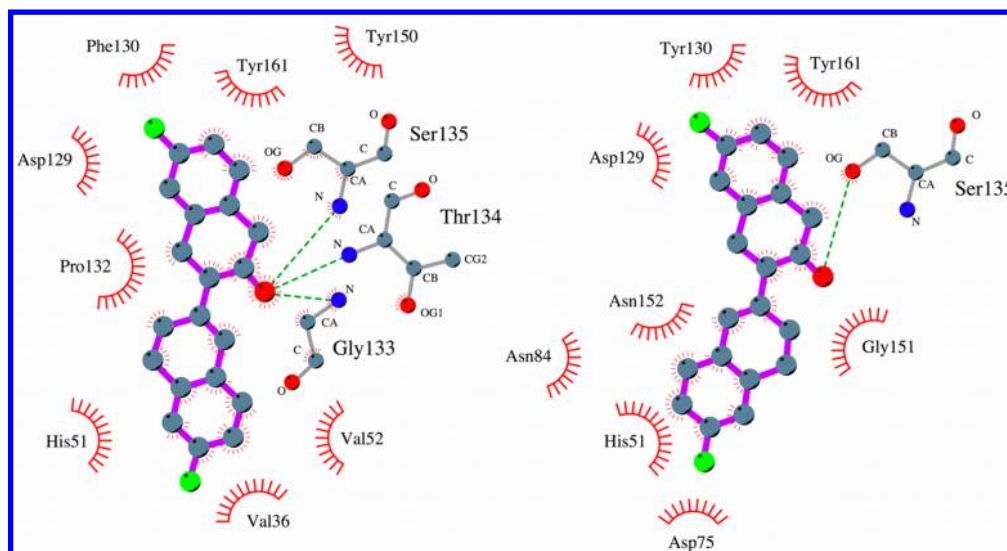


Figure 7. Comparison of intermolecular interactions between the inhibitor ZINC04321905 (purple bonds) and NS2B-NS3pro proteases from related flaviviruses. (A) ZINC04321905 bound to DEN3V NS2B-NS3pro (PDB structure 3U1J). (B) ZINC04321905 bound to WNV NS2B-NS3pro (PDB structure 2FP7). Orientations of the bound inhibitor were calculated with the Vina docking program. Hydrogen bonds and hydrophobic interactions are represented by green dashes and red hashed lines, respectively. Residue names and numbering refer to the NS2B-NS3pro. Images were prepared with LigPlot+.⁵¹

libraries are available for immediate purchase from established chemical companies, which facilitates rapid validation of high-scoring hits from virtual screening experiments. An inhibitor with very low micromolar activity against DENV protease was presented as a “proof-of-concept”, or an example that experimentally validated leads could be rapidly discovered using this portal and its integrated druglike commercially available libraries. Moreover, the identified novel small-molecule inhibitor had activity against the WNV protease, suggesting that the development of pan-flavivirus inhibitors may be possible. On the basis of its low molecular weight and absence of chemical groups associated with adverse pharmacological risk, the identified lead is a promising candidate for further in vitro testing and characterization as a potential pan-dengue antiviral drug.

AUTHOR INFORMATION

Corresponding Author

*E-mail: watowich@xray.utmb.edu.

Notes

The authors declare no competing financial interest.

ACKNOWLEDGMENTS

We thank IBM International Foundation and IBM World Community Grid for support and access to computing resources. In addition, we thank members of the Texas Advanced Computing Center (Dr. John Boisseau, Director) for providing access to TACC computing resources and assistance. Dr. John Irwin graciously provided virtual libraries, and Drs. Arthur Olson and Oleg Trott provided Autodock Vina and AutoDockTools software.

REFERENCES

- (1) Anderson, A. C. The Process of Structure-Based Drug Design. *Chem. Biol.* **2003**, *10*, 787–797.
- (2) Guida, W. C. Software for Structure-Based Drug Design. *Curr. Opin. Struct. Biol.* **1994**, *4*, 777–781.
- (3) Tomlinson, S. M.; Malmstrom, R. D.; Russo, A.; Mueller, N.; Pang, Y. P.; Watowich, S. J. Structure-Based Discovery of Dengue Virus Protease Inhibitors. *Antiviral Res.* **2009**, *82*, 110–114.
- (4) Verlinde, C. L.; Hol, W. G. Structure-Based Drug Design: Progress, Results and Challenges. *Structure* **1994**, *2*, 577–587.
- (5) Kitchen, D. B.; Decornez, H.; Furr, J. R.; Bajorath, J. Docking and Scoring in Virtual Screening for Drug Discovery: Methods and Applications. *Nat. Rev. Drug Discovery* **2004**, *3*, 935–949.
- (6) Lengauer, T.; Rarey, M. Computational Methods for Biomolecular Docking. *Curr. Opin. Struct. Biol.* **1996**, *6*, 402–406.
- (7) Seifert, M. H.; Lang, M. Essential Factors for Successful Virtual Screening. *Mini-Rev. Med. Chem.* **2008**, *8*, 63–72.
- (8) Trott, O.; Olson, A. J. AutoDock Vina: Improving the Speed and Accuracy of Docking with a New Scoring Function, Efficient Optimization, and Multithreading. *J. Comput. Chem.* **2009**, *31*, 455–461.
- (9) Wang, R.; Fang, X.; Lu, Y.; Wang, S. The PDBbind Database: Collection of Binding Affinities for Protein–Ligand Complexes with Known Three-Dimensional Structures. *J. Med. Chem.* **2004**, *47*, 2977–2980.
- (10) Wang, R.; Fang, X.; Lu, Y.; Yang, C. Y.; Wang, S. The PDBbind Database: Methodologies and Updates. *J. Med. Chem.* **2005**, *48*, 4111–4119.
- (11) World Health Organization. World Health Report. Executive Summary. Insect-Borne Diseases. www.who.int/whr/1996/media_centre/executive_summary1/en/index9.html (accessed Dec 5, 2012).
- (12) World Health Organization. Global Alert and Response (GAR): Impact of Dengue. <http://www.who.int/csr/disease/dengue/impact/en/> (accessed Nov 20, 2012).
- (13) Bhatt, S.; Gething, P. W.; Brady, O. J.; Messina, J. P.; Farlow, A. W.; Moyes, C. L.; Drake, J. M.; Brownstein, J. S.; Hoen, A. G.; Sankoh, O.; Myers, M. F.; George, D. B.; Jaenisch, T.; Wint, G. R.; Simmons, C. P.; Scott, T. W.; Farrar, J. J.; Hay, S. I. The Global Distribution and Burden of Dengue. *Nature* **2013**, *496*, 504–507.
- (14) Tomlinson, S. M.; Malmstrom, R. D.; Watowich, S. J. New Approaches to Structure-Based Discovery of Dengue Protease Inhibitors. *Infect. Disord.: Drug Targets* **2009**, *9*, 327–343.
- (15) De Clercq, E. Anti-HIV Drugs: 25 Compounds Approved within 25 Years after the Discovery of HIV. *Int. J. Antimicrob. Agents* **2009**, *33*, 307–320.
- (16) Lin, K.; Perni, R. B.; Kwong, A. D.; Lin, C. VX-950, a Novel Hepatitis C Virus (HCV) NS3-4A Protease Inhibitor, Exhibits Potent

Antiviral Activities in HCV Replicon Cells. *Antimicrob. Agents Chemother.* **2006**, *50*, 1813–1822.

(17) Sarrazin, C.; Rouzier, R.; Wagner, F.; Forestier, N.; Larrey, D.; Gupta, S. K.; Hussain, M.; Shah, A.; Cutler, D.; Zhang, J.; Zeuzem, S. SCH 503034, a Novel Hepatitis C Virus Protease Inhibitor, Plus Pegylated Interferon α -2b for Genotype 1 Nonresponders. *Gastroenterology* **2007**, *132*, 1270–1278.

(18) Natarajan, S. NS3 Protease from Flavivirus as a Target for Designing Antiviral Inhibitors against Dengue Virus. *Genet. Mol. Biol.* **2010**, *33*, 214–219.

(19) Li, J.; Lim, S. P.; Beer, D.; Patel, V.; Wen, D.; Tumanut, C.; Tully, D. C.; Williams, J. A.; Jiricek, J.; Priestle, J. P.; Harris, J. L.; Vasudevan, S. G. Functional Profiling of Recombinant NS3 Proteases from All Four Serotypes of Dengue Virus Using Tetrapeptide and Octapeptide Substrate Libraries. *J. Biol. Chem.* **2005**, *280*, 28766–28774.

(20) Aravapalli, S.; Lai, H.; Teramoto, T.; Alliston, K. R.; Lushington, G. H.; Ferguson, E. L.; Padmanabhan, R.; Groutas, W. C. Inhibitors of Dengue Virus and West Nile Virus Proteases Based on the Aminobenzamide Scaffold. *Bioorg. Med. Chem.* **2012**, *20*, 4140–4148.

(21) Frimayanti, N.; Chee, C. F.; Zain, S. M.; Rahman, N. A. Design of New Competitive Dengue NS2b/NS3 Protease Inhibitors—A Computational Approach. *Int. J. Mol. Sci.* **2011**, *12*, 1089–1100.

(22) Hsu, Y. C.; Chen, N. C.; Chen, P. C.; Wang, C. C.; Cheng, W. C.; Wu, H. N. Identification of a Small-Molecule Inhibitor of Dengue Virus Using a Replicon System. *Arch. Virol.* **2012**, *157*, 681–688.

(23) Knehans, T.; Schuller, A.; Doan, D. N.; Nacro, K.; Hill, J.; Guntert, P.; Madhusudhan, M. S.; Weil, T.; Vasudevan, S. G. Structure-Guided Fragment-Based In Silico Drug Design of Dengue Protease Inhibitors. *J. Comput.-Aided Mol. Des.* **2011**, *25*, 263–274.

(24) McCormick, K. D.; Liu, S.; Jacobs, J. L.; Marques, E. T., Jr.; Sluis-Cremer, N.; Wang, T. Development of a Robust Cytopathic Effect-Based High-Throughput Screening Assay To Identify Novel Inhibitors of Dengue Virus. *Antimicrob. Agents Chemother.* **2012**, *56*, 3399–3401.

(25) Tomlinson, S. M.; Watowich, S. J. Anthracene-Based Inhibitors of Dengue Virus NS2B-NS3 Protease. *Antiviral Res.* **2011**, *89*, 127–135.

(26) Yang, C. C.; Hsieh, Y. C.; Lee, S. J.; Wu, S. H.; Liao, C. L.; Tsao, C. H.; Chao, Y. S.; Chern, J. H.; Wu, C. P.; Yueh, A. Novel Dengue Virus-Specific NS2B/NS3 Protease Inhibitor, BP2109, Discovered by a High-Throughput Screening Assay. *Antimicrob. Agents Chemother.* **2011**, *55*, 229–238.

(27) Berman, H.; Henrick, K.; Nakamura, H. Announcing the Worldwide Protein Data Bank. *Nat. Struct. Biol.* **2003**, *10*, 980.

(28) Berman, H. M.; Westbrook, J.; Feng, Z.; Gilliland, G.; Bhat, T. N.; Weissig, H.; Shindyalov, I. N.; Bourne, P. E. The Protein Data Bank. *Nucleic Acids Res.* **2000**, *28*, 235–242.

(29) Bernstein, F. C.; Koetzle, T. F.; Williams, G. J.; Meyer, E. F., Jr.; Brice, M. D.; Rodgers, J. R.; Kennard, O.; Shimanouchi, T.; Tasumi, M. The Protein Data Bank: A Computer-Based Archival File for Macromolecular Structures. *J. Mol. Biol.* **1977**, *112*, 535–542.

(30) Erbel, P.; Schiering, N.; D'Arcy, A.; Renatus, M.; Kroemer, M.; Lim, S. P.; Yin, Z.; Keller, T. H.; Vasudevan, S. G.; Hommel, U. Structural Basis for the Activation of Flaviviral NS3 Proteases from Dengue and West Nile Virus. *Nat. Struct. Mol. Biol.* **2006**, *13*, 372–373.

(31) Noble, C. G.; Seh, C. C.; Chao, A. T.; Shi, P. Y. Ligand-Bound Structures of the Dengue Virus Protease Reveal the Active Conformation. *J. Virol.* **2012**, *86*, 438–446.

(32) Sanner, M. F. Python: A Programming Language for Software Integration and Development. *J. Mol. Graphics Modell.* **1999**, *17*, 57–61.

(33) Irwin, J. J.; Shoichet, B. K. ZINC—A Free Database of Commercially Available Compounds for Virtual Screening. *J. Chem. Inf. Model.* **2005**, *45*, 177–182.

(34) Tomlinson, S. M.; Watowich, S. J. Use of Parallel Validation High-Throughput Screens To Reduce False Positives and Identify

Novel Dengue NS2B-NS3 Protease Inhibitors. *Antiviral Res.* **2012**, *93*, 245–252.

(35) Tomlinson, S. M.; Watowich, S. J. Substrate Inhibition Kinetic Model for West Nile Virus NS2B-NS3 Protease. *Biochemistry* **2008**, *47*, 11763–11770.

(36) Kuzmic, P. Program DynaFit for the Analysis of Enzyme Kinetic Data: Application to HIV Proteinase. *Anal. Biochem.* **1996**, *237*, 260–273.

(37) Kuzmic, P. DynaFit—A Software Package for Enzymology. *Methods Enzymol.* **2009**, *467*, 247–280.

(38) Kuzmic, P.; Hill, C.; Janc, J. W. Practical Robust Fit of Enzyme Inhibition Data. *Methods Enzymol.* **2004**, *383*, 366–381.

(39) Tsai, T. Y.; Chang, K. W.; Chen, C. Y. iScreen: World's First Cloud-Computing Web Server for Virtual Screening and de Novo Drug Design Based on TCM Database@Taiwan. *J. Comput.-Aided Mol. Des.* **2011**, *25*, 525–531.

(40) Irwin, J. J.; Shoichet, B. K.; Mysinger, M. M.; Huang, N.; Colizzi, F.; Wassam, P.; Cao, Y. Automated Docking Screens: A Feasibility Study. *J. Med. Chem.* **2009**, *52*, 5712–5720.

(41) Su, X. C.; Ozawa, K.; Qi, R.; Vasudevan, S. G.; Lim, S. P.; Otting, G. NMR Analysis of the Dynamic Exchange of the NS2B Cofactor between Open and Closed Conformations of the West Nile Virus NS2B-NS3 Protease. *PLoS Neglected Trop. Dis.* **2009**, *3*, No. e561.

(42) Johnson, K. A. Fitting Enzyme Kinetic Data with KinTek Global Kinetic Explorer. *Methods Enzymol.* **2009**, *467*, 601–626.

(43) Kakkar, T.; Boxenbaum, H.; Mayersohn, M. Estimation of K_i in a Competitive Enzyme-Inhibition Model: Comparisons among Three Methods of Data Analysis. *Drug Metab. Dispos.* **1999**, *27*, 756–762.

(44) Briggs, G. E.; Haldane, J. B. S. A Note on the Kinetics of Enzyme Action. *Biochem. J.* **1925**, *19*, 338–339.

(45) Lineweaver, H.; Burk, D. The Determination of Enzyme Dissociation Constants. *J. Am. Chem. Soc.* **1934**, *56*, 658–666.

(46) Michaelis, L.; Menten, M. L. Die Kinetik der Invertinwirkung. *Biochem. Z.* **1913**, *49*, 333–369.

(47) Michaelis, L.; Menten, M. L.; Johnson, K. A.; Goody, R. S. The Original Michaelis Constant: Translation of the 1913 Michaelis–Menten Paper. *Biochemistry* **2011**, *50*, 8264–8269.

(48) Guex, N.; Peitsch, M. C. SWISS-MODEL and the Swiss-PDBViewer: An Environment for Comparative Protein Modeling. *Electrophoresis* **1997**, *18*, 2714–2723.

(49) The PyMOL Molecular Graphics System, version 1.5.0.4; Schrödinger, LLC: New York, 2010.

(50) Hulsen, T.; de Vlieg, J.; Alkema, W. BioVenn—A Web Application for the Comparison and Visualization of Biological Lists Using Area-Proportional Venn Diagrams. *BMC Genomics* **2008**, *9*, 488.

(51) Laskowski, R. A.; Swindells, M. B. LigPlot+: Multiple Ligand–Protein Interaction Diagrams for Drug Discovery. *J. Chem. Inf. Model.* **2011**, *51*, 2778–2786.